Regular paper | Journal of the KIECS. pp. 995-1002, vol. 15, no. 6, Dec. 31. 2020, t. 104, pISSN 1975-8170 | eISSN 2288-2189
http://dx.doi.org/10.13067/JKIECS.2020.15.6.995

BPSK 변조의 최대 전송률 분석: 상관 정보원의 비직교 다중 접속 관점에서

정규혁*

Analysis of Achievable Data Rate under BPSK Modulation: CIS NOMA Perspective

Kyu-Hyuk Chung*

요 약

본 논문은 연속 가우시안 입력 변조를 사용하는 대부분의 기존 NOMA 설계와는 대조적으로, BPSK 변조하에서 상관 정보원의 NOMA에 대한 최대 전송률을 분석한다. 먼저, BPSK 변조와 상관 정보원의 NOMA에 대한 최대 전송률의 폐쇄형 표현식을 유도한다. 다음, 수치적 결과를 통해, 강 채널 사용자에 대해서는, 독립 정보원의 최대 전송률과 비교하여, 상관 정보원의 최대 전송률이 감소하는 것을 보여준다. 또한, 약 채널 사용자에 대해서는, 독립 정보원의 최대 전송률과 비교하여, 상관 정보원의 최대 전송률이 증가하는 것을 입증한다. 추가로, 수신 신호와 사용자 간 간섭의 확률 분포 함수의 심도 있는 분석을 통해 이론적 결과를 입증한다.

ABSTRACT

This paper investigates the achievable data rate for non-orthogonal multiple access(NOMA) with correlated information sources(CIS), under the binary phase shift keying(BPSK) modulation, in contrast to most of the existing NOMA designs using continuous Gaussian input modulations. First, the closed-form expression for the achievable data rate of NOMA with CIS and BPSK is derived, for both users. Then it is shown by numerical results that for the stronger channel user, the achievable data rate of CIS reduces, compared with that of independent information sources(IIS). We also demonstrate that for the weaker channel user, the achievable data rate of CIS increases, compared with that of IIS. In addition, the intensive analyses of the probability density function(PDF) of the observation and the inter-user interferennce(IUI) are provided to verify our theoretical results.

키워드

NOMA, Superposition Coding, Successive Interference Cancellation, Power Allocation, Correlation Coefficient, BPSK
비직교 다중 접속, 중첩 코딩, 순차적 간섭 제거, 전력 할당, 상관 관계 계수, BPSK

Ⅰ. Introduction

Recently, non-orthogonal multiple access(NOMA) has emerged as a key enabling multiple access(MA) technology to meet the unprecedented requirements of forthcoming future fifth-generation(5G) wireless mobile networks, due to high spectral efficiency, massive connectivity, and low transmission latency[1, 2], compared to orthogonal multiple access(OMA)[3-5]. In this paper, we

* 교신저자 : 단국대학교 소프트웨어학과
• 접 수 일 : 2020. 09. 13
• 수정완료일 : 2020. 11. 01
• 게재확정일 : 2020. 12. 15
• Received : Sep. 17, 2020, Revised : Nov. 01, 2020, Accepted : Dec. 15, 2020
• Corresponding Author : Kyu-Hyuk Chung
Dept. Software Science, Dankook University,
Email : khchung@dankook.ac.kr

mainly consider the power-domain NOMA[6, 7]. The users with better channel conditions can eliminate other users' messages by applying successive interference cancellation(SIC) before decoding their own messages[8].

Lately, the bit-error rate(BER) performance of NOMA was analyzed[9]. The impacts of local oscillator imperfection for NOMA were studied[10]. In addition, the BER expression with randomly generated signals was derived[11]. The BER expression for the two and three-user cases was studied[12]. The average symbol error rate(SER) expressions for the two-user case were considered in[13].

As the state-of-the-art advances in NOMA, the optimal power control was investigated based on individual QoS constraints[14], whereas the energy harvesting in NOMA was studied for machine-to-machine(M2M) communications[15].

As in the above-mentioned literature, in NOMA, information sources are assumed to be independent, i.e., independent information sources(IIS). However, sometimes the common information needs to be transmitted. For example, many mobile game users are enjoying the mobile game together, in the same cell of 5G networks. In this case, game companies need to broadcast the screen of live players. Then such data can be modeled as correlated information sources(CIS)[16].

In this paper, we investigate the achievable data rate of NOMA for CIS, especially under the binary phase shift keying(BPSK) modulation, in contrast to most of the existing NOMA designs using continuous Gaussian input distributions. Fist, we derive the analytical expression for the achievable data rate of NOMA for CIS, for both users, respectively. Then it is shown that the achievable data rate of the stronger channel user in NOMA for CIS decreases, compared to that for IIS, whereas the achievable data rate of the weaker channel user in NOMA for CIS increases, compared to that for IIS.

The remainder of this paper is organized as follows. In Section II, the system and channel model are described. The analytical expression for the achievable data rate of NOMA for CIS is derived in Section III. The results are presented and discussed in Section IV. Finally, the conclusions are presented in Section V.

II. System and Channel Model

In a cellular downlink NOMA transmission system, all the users are assumed to be experiencing block fading, in a narrow band of frequencies. For wideband systems, orthogonal frequency division multiplexing(OFDM) can transform a frequency-selective channel into slow fading ones. A base station and paired users are within the cell. The complex channel coefficient between the mth user and the base station is denoted by h_m, $m=1,2$. The channels are sorted as $|h_1| > |h_2|$. The base station sends the superimposed signal $x=\sqrt{\alpha P_A}\,s_1+\sqrt{(1-\alpha)P_A}\,s_2$, where s_m is the message for the mth user with unit power, $E[|s_1|^2]=E[|s_2|^2]=1$, where $E[u]$ represents the expectation of the random variable(RV) u, α is the power allocation factor, with $0\le\alpha\le 1$, and P_A is the total allocated power. The correlation coefficient is $\rho_{1,2}=E[s_1 s_2^*]$. Owing to correlation, the power of the superimposed signal x is not equal to P_A. Therefore, for the constant total transmitted power P at the base station, P_A is effectively scaled by[17]

$$P_A=\frac{P}{1+2Re\{\rho_{1,2}\}\sqrt{\alpha}\sqrt{1-\alpha}} \tag{1}$$

where $Re\{z\}$ is the real part of a complex number z. It should be noted that for IIS, $P_A=P$. The observation at the mth user is given by

$$r_m = |h_m| x + n_m \quad (2)$$
$$= |h_m| \sqrt{\alpha P_A} s_1 + |h_m| \sqrt{(1-\alpha)P_A} s_2 + n_m,$$

where $n_m \sim N(0, N_0/2)$ is additive white Gaussian noise(AWGN). The notation $N(\mu, \Sigma)$ represents the distribution of a Gaussian RV with mean μ and variance Σ. Two uniform sources are given by

$$\begin{cases} P(b_1 = 0) = p_1 = 1/2 \\ P(b_1 = 1) = 1 - p_1 = 1/2 \end{cases} \quad (3)$$

$$\begin{cases} P(b_2 = 0) = p_2 = 1/2 \\ P(b_2 = 1) = 1 - p_2 = 1/2 \end{cases}.$$

For IIS, the joint probability mass function (PMF) is given by

$$\begin{cases} P(b_1 = 0, b_2 = 0) = \frac{1}{2} \times \frac{1}{2} = \frac{1}{4} \\ P(b_1 = 0, b_2 = 1) = \frac{1}{2} \times \frac{1}{2} = \frac{1}{4} \\ P(b_1 = 1, b_2 = 0) = \frac{1}{2} \times \frac{1}{2} = \frac{1}{4} \\ P(b_1 = 1, b_2 = 1) = \frac{1}{2} \times \frac{1}{2} = \frac{1}{4}. \end{cases} \quad (4)$$

For CIS, the joint PMF is given by

$$\begin{cases} P(b_1 = 0, b_2 = 0) = q_{0,0} \\ P(b_1 = 0, b_2 = 1) = q_{0,1} = \frac{1}{2} - q_{0,0} \\ P(b_1 = 1, b_2 = 0) = q_{1,0} = \frac{1}{2} - q_{0,0} \\ P(b_1 = 1, b_2 = 1) = q_{1,1} = q_{0,0}. \end{cases} \quad (5)$$

In this paper, we assume that CIS has the positive correlation, $\rho_{1,2} > 0$, which corresponds to $\frac{1}{4} < q_{0,0} < \frac{1}{2}$. Then the correlation coefficient is calculated as[16]

$$\rho_{1,2} = E[s_1 s_2^*] = 4q_{0,0} - 1. \quad (6)$$

In this paper, we consider the BPSK modulation, $s_m \in \{+1, -1\}$, and to ensure the user fairness, we consider the power allocation range, $\alpha \le 0.5$. It is also assumed that the conventional bit-to-symbol mapping:

$$\begin{cases} s_1(b_1 = 0) = +1 \\ s_1(b_1 = 1) = -1 \end{cases} \quad \begin{cases} s_2(b_2 = 0) = +1 \\ s_2(b_2 = 1) = -1. \end{cases} \quad (7)$$

III. Derivation of Achievable Data Rate

Shannon originally defined the channel capacity as the mutual information $I(y;x) = h(y) - h(y \mid x)$, where $h(y) = -E[\log_2 p_Y(y)]$ is the differential entropy, and $p_Y(y)$ is the probability density function (PDF). We start the derivation from the above-mentioned definition.

First, if the perfect SIC is assumed, the achievable data rate R_1 is given by

$$R_1 = I(r_1; b_1 \mid b_2) \quad (8)$$
$$= h(r_1 \mid b_2) - h(r_1 \mid b_1, b_2).$$

Then, the conditional differential entropy $h(r_1 \mid b_2)$ is calculated by

$$\begin{aligned} & h(r_1 \mid b_2) \quad (9) \\ &= h\left(|h_m| \sqrt{\alpha P_A} s_1(b_1) + |h_m| \sqrt{(1-\alpha)P_A} s_2(b_2) + n_1 \mid b_2 \right) \\ &= h\left(|h_m| \sqrt{\alpha P_A} s_1(b_1) + n_m \mid b_2 \right) \\ &= h(y_1 \mid b_2), \end{aligned}$$

where $y_1 = |h_m| \sqrt{\alpha P_A} s_1(b_1) + n_m$ is the observation after SIC is performed on r_1. Then, the conditional PDF of $P_{Y_1 \mid B_2}(y_1 \mid b_2)$ is represented by

$$P_{Y_1 \mid B_2}(y_1 \mid b_2) = \quad (10)$$
$$\frac{q_{0,b_2}}{P(b_2)} \frac{1}{\sqrt{2\pi N_0/2}} e^{-\frac{(r_1 - |h_1|\sqrt{P_A \alpha})^2}{2N_0/2}}$$
$$+ \frac{q_{1,b_2}}{P(b_2)} \frac{1}{\sqrt{2\pi N_0/2}} e^{-\frac{(r_1 + |h_1|\sqrt{P_A \alpha})^2}{2N_0/2}}.$$

Thus the differential entropy is calculated by

$$\begin{aligned} & h(y_1 \mid b_2) \\ &= -E[\log_2 P_{Y_1 \mid B_2}(y_1 \mid b_2)] \\ &= -\sum_{b_2=0}^{1} P(b_2) \int_{-\infty}^{+\infty} P_{Y_1 \mid B_2}(y_1 \mid b_2) \log_2 P_{Y_1 \mid B_2}(y_1 \mid b_2) dy_2 \\ &= -\int_{-\infty}^{+\infty} P_{Y_1 \mid B_2}(y_1 \mid b_2 = 0) \log_2 P_{Y_1 \mid B_2}(y_1 \mid b_2 = 0) dy_2. \end{aligned} \tag{11}$$

And the conditional differential entropy $h(r_1 \mid b_1, b_2)$ is calculated by

$$\begin{aligned} & h(r_1 \mid b_1, b_2) \\ &= h\left(\mid h_m \mid \sqrt{\alpha P_A}\, s_1(b_1) + \mid h_m \mid \sqrt{(1-\alpha) P_A}\, s_2(b_2) + n_1 \mid b_1, b_2 \right) \\ &= h(n_1 \mid b_1, b_2) \\ &= h(n_1) \\ &= \frac{1}{2} log_2(2\pi e N_0/2). \end{aligned} \tag{12}$$

Second, the PDF of y_2 is represented by

$$\begin{aligned} P_{Y_2}(y_2) = {} & q_{0,0} \frac{1}{\sqrt{2\pi N_0/2}} e^{-\frac{\left(r_2 - |h_2|\left(+\sqrt{P_A(1-\alpha)} + \sqrt{P_A \alpha}\right)\right)^2}{2N_0/2}} \\ & + q_{0,1} \frac{1}{\sqrt{2\pi N_0/2}} e^{-\frac{\left(r_2 - |h_2|\left(-\sqrt{P_A(1-\alpha)} + \sqrt{P_A \alpha}\right)\right)^2}{2N_0/2}} \\ & + q_{1,0} \frac{1}{\sqrt{2\pi N_0/2}} e^{-\frac{\left(r_2 - |h_2|\left(+\sqrt{P_A(1-\alpha)} - \sqrt{P_A \alpha}\right)\right)^2}{2N_0/2}} \\ & + q_{1,1} \frac{1}{\sqrt{2\pi N_0/2}} e^{-\frac{\left(r_2 - |h_2|\left(-\sqrt{P_A(1-\alpha)} - \sqrt{P_A \alpha}\right)\right)^2}{2N}} \end{aligned} \tag{13}$$

It should be noted that for the second user, since SIC cannot be performed, we have the received signal

$$y_2 = r_2. \tag{14}$$

Then, the differential entropy is calculated by

$$\begin{aligned} h(y_2) &= -E[\log_2 P_{Y_2}(y_2)] \\ &= -\int_{-\infty}^{+\infty} P_{Y_2}(y_2) \log_2 P_{Y_2}(y_2) dy_2. \end{aligned} \tag{15}$$

And the conditional differential entropy is calculated by

$$\begin{aligned} h(y_2 \mid b_2) &= -E[\log_2 P_{Y_2 \mid B_2}(y_2 \mid b_2)] \\ &= -\sum_{b_2=0}^{1} P(b_2) \int_{-\infty}^{+\infty} P_{Y_2 \mid B_2}(y_2 \mid b_2) \log_2 P_{Y_2 \mid B_2}(y_2 \mid b_2) dy_2. \end{aligned} \tag{16}$$

where the conditional PDF is given by

$$\begin{aligned} & P_{Y_2 \mid B_2}(y_2 \mid b_2) = \\ & + \frac{q_{0,b_2}}{P(b_2)} \frac{1}{\sqrt{2\pi N_0/2}} e^{-\frac{\left(r_2 - |h_2|\left(+(-1)^{b_2}\sqrt{P_A(1-\alpha)} + \sqrt{P_A \alpha}\right)\right)^2}{2N_0/2}} \\ & + \frac{q_{1,b_2}}{P(b_2)} \frac{1}{\sqrt{2\pi N_0/2}} e^{-\frac{\left(r_2 - |h_2|\left(+(-1)^{b_2}\sqrt{P_A(1-\alpha)} - \sqrt{P_A \alpha}\right)\right)^2}{2N_0/2}}. \end{aligned} \tag{17}$$

Then we have the achievable data rate R_2 for the second user

$$\begin{aligned} R_2 &= h(y_2) - h(y_2 \mid b_2) \\ &= h(y_2) + \sum_{b_2=0}^{1} P(b_2) \int_{-\infty}^{+\infty} P_{Y_2 \mid B_2}(y_2 \mid b_2) \log_2 P_{Y_2 \mid B_2}(y_2 \mid b_2) dy_2 \\ &= h(y_2) + \int_{-\infty}^{+\infty} P_{Y_2 \mid B_2}(y_2 \mid b_2 = 0) \log_2 P_{Y_2 \mid B_2}(y_2 \mid b_2 = 0) dy_2 \\ &= -\int_{-\infty}^{+\infty} P_{Y_2}(y_2) \log_2 P_{Y_2}(y_2) dy_2 \\ &+ \int_{-\infty}^{+\infty} P_{Y_2 \mid B_2}(y_2 \mid b_2 = 0) \log_2 P_{Y_2 \mid B_2}(y_2 \mid \end{aligned} \tag{18}$$

Ⅳ. Results and Discussions

It is assumed that $\mid h_1 \mid = \sqrt{1.5}$ and $\mid h_2 \mid = \sqrt{0.5}$ We consider the constant total transmitted signal

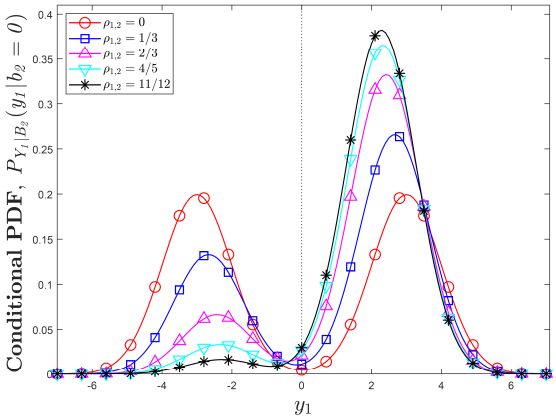

Fig. 1 Conditional PDF $P_{Y_1 \mid B_2}(y_1 \mid b_2=0)$ of observation for first user

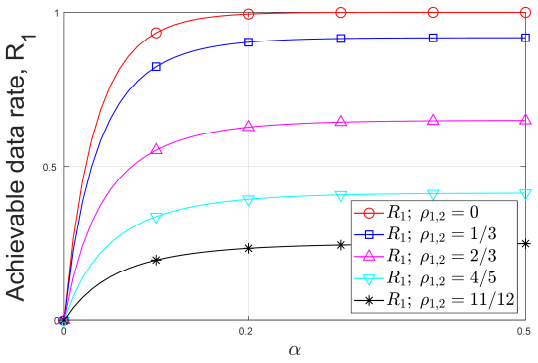

Fig. 2 Achievable data rate R_1 for first user

power to noise power ratio (SNR) $P/N_0=15$.

First, for $\alpha=0.2$, we depict the PDF of $P_{Y_1 \mid B_2}(y_1 \mid b_2=0)$ for the first user, in order to investigate the impacts of CIS, in Fig. 1, for the various correlation coefficient, $\rho_{1,2}=0, \frac{1}{3}, \frac{2}{3}, \frac{4}{5}$ and $\frac{11}{12}$, which correspond to $q_{0,0}=\frac{1}{4}, \frac{2}{6}, \frac{5}{12}, \frac{11}{24}$ and $\frac{23}{48}$, respectively. As shown in Fig. 1, when the correlation coefficient $\rho_{1,2}$ increases, the double Gaussian bell-shape signal approaches a single Gaussian bell-shape signal, i.e., the entropy decreases. This is because the correlation coefficient $\rho_{1,2}$ increases. Thus, we expect that the achievable data rate R_1 will decrease.

In Fig. 2, we plot the achievable data rate R_1, for the various correlation coefficient. As shown in Fig. 2, when the correlation coefficient $\rho_{1,2}$ increases, the achievable data rate R_1 decreases, due to the reduced entropy of the observation.

Second, in Fig. 3, the PDF of the observation $P_{Y_2}(y_2)$ for the second user is depicted for the various correlation coefficient $\rho_{1,2}$, for $\alpha=0.2$. As shown in Fig. 3, as the correlation coefficient $\rho_{1,2}$ increases, the the inter-user interference(IUI) looks like dissapearing. Also, we plot the PDF $P_{Y_2 \mid B_2}(y_2 \mid b_2=0)$ of the IUI+AWGN, in Fig. 4, for $\alpha=0.2$. As shown in Fig. 4, as the correlation coefficient $\rho_{1,2}$ increases, the IUI+AWGN approches near AWGN, i.e., the IUI becomes less severe. Thus, we expect that the achievable data rate R_2 will increase.

In Fig. 5, we plot the achievable data rate R_2, for the various correlation coefficient. As shown in Fig. 5, when the correlation coefficient $\rho_{1,2}$ increases, the achievable data rate R_1 also increases, due to the reduced IUI.

Lastly, we should metion that the results of both users are different. Specifically, this is because the achievable data rate of the stronger channel user is affected by the allocated power, whereas the achievable data rate of the weaker channel user is mainly influenced by the IUI. Physically, due to the correlation, the base station allocates less power, for the given constant total transmitted power. In addition, such correlation reduces the IUI, which determines the performance of the weaker channel user.

Ⅴ. Conclusion

This paper investigated the achievable data rate

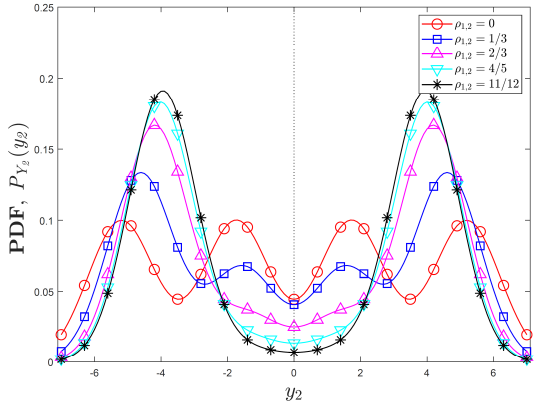

Fig. 3 PDF $P_{Y_2}(y_2)$ of observation for second user

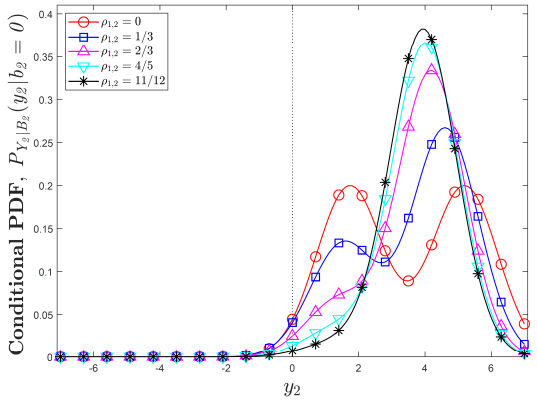

Fig. 4 Conditional PDF $P_{Y_2 \mid B_2}(y_2 \mid b_2=0)$ of IUI+AWGN for second user

for NOMA with CIS, under the BPSK modulation. First, the analytical expression for the achievable data rate of NOMA with CIS and BPSK was derived, for both users. Then it was shown that for the stronger channel user, the achievable data rate of CIS reduces, whereas for the weaker channel user, the achievable data rate of CIS increases, compared with that of IIS, respectively. In addition, we also investigated the impacts of CIS on the PDF of the observation and the IUI, for both users.

As a direction of the future research, it would be interesting to design the modulation technique in

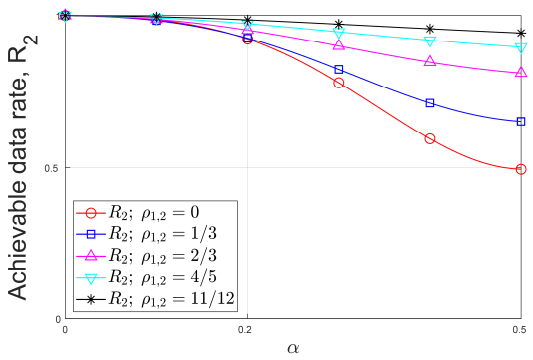

Fig. 5 Achievable data rate R_2 for second user

superposition coding for increasing the reduced achievable data rate of the stronger channel user, with a tolerable loss of the achievable data rate of the weaker channel user.

References

[1] Y. Saito, Y. Kishiyama, A. Benjebbour, T. Nakamura, A. Li, and K. Higuchi, "Non-orthogonal multiple access (NOMA) for cellular future radio access," in *Proc. IEEE 77th Veh. Technol. Conf. (VTC Spring)*, Dresden, Germany, June 2013, pp. 1-5.

[2] Z. Ding, Y. Liu, J. Choi, Q. Sun, M. Elkashlan, C.-L. I, and H. V. Poor, "Application of non-orthogonal multiple access in LTE and 5G networks," *IEEE Commun. Mag.*, vol. 55, no. 2, Feb. 2017, pp. 185-191.

[3] M.-C. Yang, "An adaptive tone reservation scheme for PAPR reduction of OFDM signals," *J. of the Korea Institute of Electronic Communication Sciences*, vol. 14, no. 5, Oct. 2019, pp. 817-824.

[4] H.-J. Ahn and M.-C. Yang, "Analysis of Automatic Neighbor Relation Technology in Self Organization Networks of LTE," *J. of the Korea Institute of Electronic Communication Sciences*, vol. 14, no. 5, Oct. 2019, pp. 893-900.

[5] K. Zhang and H.-J. Suh, "An analysis of multiuser diversity technology in the MIMO-OFDM system," *J. of the Korea Institute of Electronic Communication Sciences*, vol. 14, no. 6, Dec. 2019, pp. 1121-1128.

[6] L. Dai, B. Wang, Y. Yuan, S. Han, C.-L. I, and Z. Wang, "Non-orthogonal multiple access for 5G: Solutions, challenges, opportunities, and future research trends," *IEEE Commun. Mag.*, vol. 53, no. 9, Sept. 2015, pp. 74-81.

[7] Q. Wang, R. Zhang, L.-L. Yang, and L. Hanzo, "Non-orthogonal multiple access: A unified perspective," *IEEE Wireless Commun.*, vol. 25, no. 2, Apr. 2018, pp. 10-16.

[8] D. Wan, M. Wen, F. Ji, H. Yu, and F. Chen, "Non-orthogonal multiple access for cooperative communications: Challenges, opportunities, and trends," *IEEE Wireless Commun.*, vol. 25, no. 2, May 2018, pp. 109-117.

[9] M. Aldababsa, C. Göztepe, G. K. Kurt, and O. Kucur, "Bit error rate for NOMA network," *IEEE Commun. Lett.*, vol. 24, no. 6, June 2020, pp. 1188-1191.

[10] A.-A.-A. Boulogeorg, N. D. Chatzidiamantis, and G. K. Karagiannid, "Non-orthogonal multiple access in the presence of phase noise," *IEEE Commun. Lett.*, vol. 24, no. 5, May 2020, pp. 1133-1137.

[11] L. Bariah, S. Muhaidat, and A. Al-Dweik, "Error Probability Analysis of Non-Orthogonal Multiple Access Over Nakagami-*m* Fading Channels," *IEEE Trans. Commun.*, vol. 67, no. 2, Feb. 2019, pp. 1586-1599.

[12] T. Assaf, A. Al-Dweik, M. E. Moursi, and H. Zeineldin, "Exact BER Performance Analysis for Downlink NOMA Systems Over Nakagami-m Fading Channels," *IEEE Access*, vol. 7, 2019, pp. 134539-134555.

[13] I. Lee and J. Kim, "Average Symbol Error Rate Analysis for Non-Orthogonal Multiple Access With M-Ary QAM Signals in Rayleigh Fading Channels," *IEEE Commun. Lett.*, vol. 23, no. 8, Aug. 2019, pp. 1328-1331.

[14] Z. Yang, W. Xu, C. Pan, Y. Pan, and M. Chen, "On the optimality of power allocation for NOMA downlinks with individual QoS constraints," *IEEE Commun. Lett.*, vol. 21, no. 7, July 2017, pp. 1649-1652.

[15] Z. Yang, W. Xu, Y. Pan, C. Pan, and M. Chen, "Energy efficient resource allocation in machine-to-machine communications with multiple access and energy harvesting for IoT," *IEEE Internet Things J.*, vol. 5, no. 1, Feb. 2018, pp. 229-245.

[16] K. Chung, "Optimal Detection for NOMA systems with correlated information sources of interactive mobile users," *J. of the Korea Institute of Electronic Communication Sciences*, vol. 15, no. 4, Aug. 2020, pp. 651-657.

[17] K. Chung, "On power of correlated superposition coding in NOMA," *J. IKEEE*, vol. 24, no. 1, Mar. 2020, pp. 360-363.

저자 소개

정규혁(Kyu-Hyuk Chung)

1997년 성균관대학교 전자공학과 졸업(공학사)

1998년 Univ. of Southern California 전기공학과 졸업(공학석사)

2003년 Univ. of Southern California 전기공학과 졸업(공학박사)

2005년 ~현재 단국대학교 SW융합대학 소프트웨어학과 교수

※ 관심분야 : 5G이동통신시스템, 비직교다중접속